Journal of Global Positioning Systems (2026)
Vol. 22, Issue 2:223-238
DOI: 10.5081/jgps.22.2.223

Impacts of the Three Largest Geomagnetic Storms during 1996–2026 on Global GPS Precise Point Positioning

Bowei Liu[1,2,3], Zhizhao Liu[2,4,5,6], Jing Wu[2], Libo Liu[1,3,7] ✉, Biqiang Zhao[1,3]

1 Key Laboratory of Planetary Science and Frontier Technology, Institute of Geology and Geophysics, Chinese Academy of Sciences, Beijing, China
2 State Key Laboratory of Climate Resilience for Coastal Cities, Department of Land Surveying and Geospatial Science (LSGS), The Hong Kong Polytechnic University, Hong Kong, China
3 College of Earth and Planetary Sciences, University of Chinese Academy of Sciences, Beijing, China
4 Otto Poon Research Institute for Climate-Resilient Infrastructure (RICRI), The Hong Kong Polytechnic University, Kowloon, Hong Kong, China
5 Meteorological Observation Center, China Meteorological Administration (CMA), No. 46, Zhongguancun South Avenue, Haidian District, Beijing 100082, China
6 Department of Geomatics Engineering, Schulich School of Engineering, The University of Calgary, Calgary, Alberta, Canada, T2N 1N4
7 Heilongjiang Mohe National Observatory of Geophysics, Institute of Geology and Geophysics, Chinese Academy of Sciences, Beijing, China

✉ the Corresponding authors, Zhizhao Liu lszzliu@polyu.edu.hk and Libo Liu liul@mail.iggcas.ac.cn

Abstract: Geomagnetic storms have profound impacts on the propagation and reception of electromagnetic waves, including the signals of Global Navigation Satellite System (GNSS). This study investigates the impacts of three largest geomagnetic storms during 1996–2026 (March 2001 storm, *November 2003 storm, and May 2024 storm) on the* Global Positioning System (GPS) Precise Point Positioning (PPP) performance. We quantified the degradation of GPS positioning accuracy and service availability under geomagnetic storms based on dual-frequency kinematic PPP solutions of a global network of International GNSS Service (IGS) stations processed by the PRIDE PPP-AR software. The results indicated that high-latitude regions suffer the most significant degradation during storm main phases, with kinematic PPP Root Mean Square Errors (RMSE) increasing by a factor of approximately two compared to pre-storm levels. While the average accuracy degradation patterns were generally consistent across the three events, the "worst-case" reliability metrics (95th percentile errors) exhibited high variability, suggesting that storm intensity alone does not dictate localized extreme disturbances. Notably, the May 2024 event demonstrated a significantly lower PPP solution outage rate than the historical 2001 and 2003 events, highlighting the resilience gained from two decades of advancements in satellite technology and modern receiver hardware. Furthermore, a comparative analysis of co-located stations revealed that receiver architecture significantly affects signal tracking stability during storm main phase. These findings provide a definitive assessment of global PPP vulnerabilities under extreme space weather and offer valuable insights for the development of robust mitigation strategies for future solar maximum cycles.

Keywords: Precise Point Positioning (PPP); Geomagnetic storm; 3D positioning errors; Global Positioning System (GPS)

1. Introduction

Geomagnetic storms are the most significant disturbances in the near-space environment around the Earth. They stem from intensified solar wind activity and its dynamic coupling with the magnetosphere-

ionosphere-thermosphere system. Triggered primarily by coronal mass ejections (CMEs) and interplanetary shock waves, these events progress through distinct main storm and recovery phases, injecting substantial energy into the polar ionosphere (Kelley, 1989). This energy input drives complex ionospheric responses, including enhanced polar convection and Joule heating, effective storm-time circulation, and frequent wave transportation, which collectively alter ionospheric density, composition, and dynamics (Balan et al., 2018; Fejer, 1997; Liu et al., 2023). These storm-time responses create large-scale structures, ranging from polar cap patches and auroral blobs to equatorial plasma bubbles (EPBs), as well as small-scale irregularities spanning from hundreds of kilometers to centimeter-level ionospheric field-aligned irregularities (Abdu, 2012; Liu et al., 2026; Wernik et al., 2003). These ionospheric structures pose a critical threat to satellite-based navigation systems (Li et al., 2021; Wang et al., 2021). These structures induce rapid fluctuations in signal amplitude and phase, known as ionospheric scintillation, which can lead to a degraded signal-to-noise ratio, frequent cycle slips, and even loss of lock of GPS signals, thereby degrading the accuracy and reliability of GPS positioning services.

As the demand for high-precision positioning continues to rise, Precise Point Positioning (PPP) has emerged as a widely adopted technique that can deliver centimeter-level accuracy with a single receiver using dual-frequency code and phase observations (Zumberge et al., 1997). Standard PPP processing typically relies on the ionosphere-free combination to mitigate first-order ionospheric effects. However, this approach is probably ineffective under disturbed ionospheric conditions caused by geomagnetic storms (Yang et al., 2020). Although the ionosphere-free combination removes the first-order dispersive delay, it cannot suppress the rapid phase and amplitude fluctuations caused by small-scale ionospheric irregularities. During intense geomagnetic storms, these fluctuations can increase carrier-phase residuals, trigger frequent ambiguity resets, and cause position outages, rendering conventional ionospheric mitigation insufficient. Therefore, it is crucial to understand the performance of PPP under extreme space weather conditions.

A substantial amount of research has been dedicated to assessing the impact of geomagnetic storms on Global Navigation Satellite System (GNSS) positioning. Earlier studies also documented substantial GPS-related disturbances during extreme geomagnetic storm. For the 31 March 2001 storm, a single-frequency GPS receiver at Bear Lake Observatory experienced positioning errors of up to approximately 20 m for more than three hours (Sojka et al., 2004). Warnant et al. (2007) further identified strong degradation events in real-time kinematic GPS performance during this storm and associated them with enhanced ionospheric variability and large-scale traveling ionospheric disturbances. For the 20 November 2003 storm, Hernández-Pajares et al. (2005) showed that the storm significantly degraded ionospheric corrections, positioning accuracy, and integrity performance. Subsequent investigations reported unusually large and rapidly varying GPS ionospheric delay gradients over Europe (Stankov et al., 2009), while a global statistical analysis identified widespread GPS signal losses associated with strong total electron content (TEC) variations and ionospheric irregularities during the event (Zhang et al., 2020). The extreme geomagnetic storm occurring during May 10–11, 2024 is considered one of the most intense events of the past three decades. This event provided an opportunity to study the effects of extreme storms on the latest GNSS applications. Mid-latitude investigations (Park et al., 2025) revealed that even dual-frequency PPP solutions experienced substantial three-dimensional (3D) error increases and frequent re-convergences during this event, challenging the idea that mid-latitudes are immune to such disturbances. Global analyses (Danilchuk et al., 2025; Yang & Morton, 2025) further mapped the spatial extent of these degradations and correlated performance drops with ionospheric indices, such as the rate of TEC index (ROTI).

Despite these advancements, there are still critical gaps. Many previous global-scale analyses, such as those by Wang et al. (2020), focused primarily on single-frequency observations, which do not represent the operational robustness of modern dual-frequency PPP used in professional high-accuracy applications. Conversely, dual-frequency studies often relied on limited receiver networks or restricted their scope to specific regions (e.g., Lu et al., 2020; Zhang et al., 2025), lacking a comprehensive global perspective. Although individual extreme geomagnetic storm events have been studied, comparative research that evaluates PPP performance across multiple similar extreme events is seldom conducted. The existing literature lacks a systematic evaluation of how global PPP responds to the most severe space weather scenarios recorded in recent decades.

To address these gaps, this study conducts a comprehensive analysis of the impacts of the three largest geomagnetic storms in the period 1996–2026 on Global Positioning System (GPS) PPP. Using a global

network of International GNSS Service (IGS) stations, we employ dual-frequency ionosphere-free PPP solutions to quantify positioning accuracy degradation. By comparing these extreme events, we aim to provide a quantitative assessment of the vulnerabilities of current high-precision GPS infrastructure to severe space weather, offering valuable insights for the development of robust mitigation strategies in the upcoming solar maximum cycle.

2 . Data Description and Processing Strategies

2.1 Selection of Three Largest Geomagnetic Storm Events and GNSS Stations

To evaluate the resilience of GPS PPP under extreme space weather conditions, this study focuses on the three most intense geomagnetic storms recorded in the past three decades (1996–2026). The storms were selected based on their minimum Disturbance Storm Time (Dst) index value, which is a standard measure of ring current intensity and overall geomagnetic storm severity (Gonzalez et al., 1994). A lower (more negative) Dst index correlates with stronger magnetospheric disturbances and more severe ionospheric perturbations. Based on this criterion, the three largest events are selected and shown in Table 1.

Table 1. The three largest geomagnetic storm events during 1996–2026

Rank	Occurrence date	Minimum Dst index
First	November 20, 2003	–422 nT
Second	May 10, 2024	–412 nT
Third	March 31, 2001	–387 nT

The largest geomagnetic storm occurred on November 20, 2003, reaching a minimum Dst index of –422 nT. It occurred in the declining phase of Solar Cycle 23. This storm is notable for its intensity, as well as for the severe ionospheric scintillation and rapid TEC fluctuations observed globally (Alex et al., 2006). The second largest storm occurred on May 10, 2024, with a minimum Dst index of –412 nT. As noted in recent literature (Elvidge & Themens, 2024), this storm stands out as an exceptional extreme event of Solar Cycle 25. The third largest storm took place on March 31, 2001 during the maximum of Solar Cycle 23, recording a minimum Dst index of –387 nT. Driven by a fast coronal mass ejection (CME), the storm resulted in significant magnetospheric compression and widespread auroral expansion (Zhang et al., 2007). Both the first and the third largest geomagnetic storms occurred in Solar Cycle 23 which was more than two decades ago. The second largest geomagnetic storm occurred in 2024. Compared to two decades ago, the GPS technologies in both satellites and receivers have advanced significantly. Thus the second storm provides us the opportunity to assess the current and latest GPS infrastructure and receiver technologies under extreme conditions.

For a comparative analysis of these historical events, GNSS observation data were primarily sourced from the global tracking network of the IGS. The selection of GNSS stations adhered to the following criteria to ensure the reliability and comparability of PPP results across a 30-year span:

1. Data continuity and quality: Only stations with providing continuous dual-frequency observation data throughout each storm event (pre-storm, storm main phase, and storm recovery phase) were selected, to enable ionosphere-free combination processing. Given the temporal span of the study, data quality control was applied to exclude stations with high noise levels or frequent signal interruptions unrelated to storm activity.

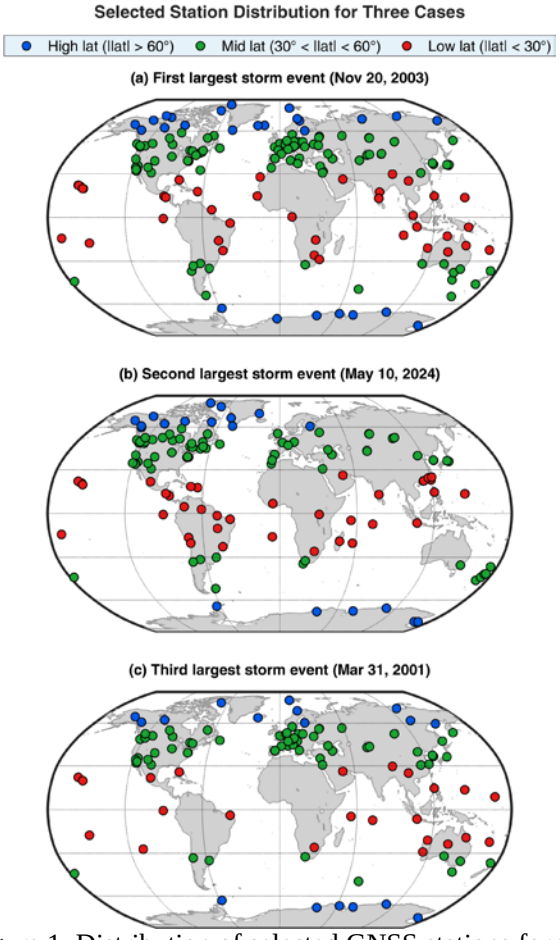

Figure 1. Distribution of selected GNSS stations for the November 2003, May 2024, and March 2001 geomagnetic storm events.

2. Precise reference coordinates: To accurately quantify the positioning errors of the PPP solutions, high-precision reference coordinates are essential. For each selected station, the "ground truth" coordinates were obtained from the IGS Site Independent Exchange (SINEX) files. These weekly combined solutions provide consistent, millimeter-level accuracy coordinates, serving as the definitive benchmark for evaluating PPP performance degradation during the storm events.

The processing period for each event encompasses a 10-day window centered on the main phase of the storm. This includes four quiet days prior to the storm onset (serving as a baseline for nominal positioning accuracy), the storm main phase, and the subsequent storm recovery phase. Such an extended processing period allows for a comparative assessment of positioning degradation during geomagnetic storm disturbance when compared to pre-storm time. The distribution of selected GNSS stations in the three storm events is shown in Figure 1, with more than 100 stations for each storm event.

2.2 Processing Strategy for Kinematic PPP

We employed the kinematic PPP approach to evaluate the impacts of extreme geomagnetic storms on GPS positioning accuracy before storm, during the storm main phase, and during the storm recovery phase. The dual-frequency GPS pseudorange and carrier phase measurements are processed using the PRIDE PPP-AR (Geng et al., 2019), an open-source GNSS data processing software developed by PRIDE laboratory at the GNSS Center of Wuhan University, China. The software supports the processing of GNSS data from multiple constellations (GPS, GLONASS, Galileo, BDS-2/3, QZSS) with full-frequency/dual-frequency ionosphere-free combinations. The main processing strategy of kinematic PPP used in this study is summarized in Table 2. A critical aspect of the processing strategy is about the selection of satellite constellations. Despite the availability of multi-constellation signals during the May 2024 event, we limited the processing to GPS satellite signals only for all three storm events. This is because for both March 2001 and November 2003 events, other GNSS constellations (e.g., GLONASS, Galileo, and BeiDou) were not well developed. Therefore, only GPS constellation was selected for consistent comparability purposes across the three decades.

Table 2. Summary of processing strategies used in the kinematic PPP.

Item	Processing strategy
GNSS signals	GPS: L1/L2
GNSS observations	Pseudorange and carrier phase measurements
Positioning mode	PPP-kinematic
Sampling interval	30 s
Elevation mask angle	15°
Satellite orbit and clock	Precise orbits and clocks products from WHU
Ionospheric delay	Ionosphere-Free combination
Troposphere delay	Piece-wise constant for 60 minutes
Phase Center corrections	IGS ATX files
Cycle slip detection	Geometry-Free and Melbourne-Wubbena combination
Ambiguity	Float solution

3.Results

3.1 Geophysical Conditions of the Three Storm Events

To understand the severity of the geophysical conditions during the three selected geomagnetic storms, the temporal variations of two key geomagnetic indices, Dst and Kp, were depicted in Figure 2. The Dst index primarily monitors the intensity of the ring current, serving as a proxy for the overall magnitude of a geomagnetic storm (Gonzalez et al., 1994). The Kp index characterizes global geomagnetic disturbances, particularly indicating the energy input from the solar wind to Earth's magnetosphere and ionosphere (Bartels et al., 1939; Tanskanen et al., 2005). An intense geomagnetic storm typically undergoes a distinct four-phase structure (Tsurutani & Gonzalez, 1997), which

provides the temporal framework for our analysis: the pre-storm period, storm initial phase, storm main phase, and storm recovery phase. Pre-storm period precedes the onset of the storm and is generally in a stable state, serving as the baseline for comparing with subsequent disturbances. Storm initial phase is characterized by a sharp increase in the Dst index, i.e., Sudden Storm Commencement (SSC). The initial phase was not evaluated as a separate statistical interval because it is brief and its boundaries are not consistently identifiable across all three events. These transition epochs were excluded from the phase-based comparisons; therefore, Figure 2 highlights only the pre-storm, main, and recovery intervals used in the subsequent analyses. Following the initial phase, the main phase is defined by the intense injection of energy into the magnetosphere, leading to the enhancement of the ring current (Kamide et al., 1998). This is the most dynamic period of the storm (Kelley, 1989), characterized by a rapid and significant decrease in the Dst index. As the energy injection subsides, the ring current begins to decay, and the geomagnetic field gradually returns to its quiet state (Tsurutani et al., 2006). The storm recovery phase is characterized by a recovery of the Dst index towards zero. In this study, we define the recovery phase window as the period from the Dst minimum to the point where the Dst index recovers to –50 nT. The –50 nT threshold is conventionally used as the lower bound for identifying a geomagnetic storm (Gonzalez et al., 1994). Values above this threshold generally indicate non-storm or only weakly disturbed conditions. Accordingly, the influence on GPS PPP is expected to diminish substantially as ionospheric conditions stabilize.

The November 2003 event occurred during the declining phase of Solar Cycle 23 with a maximum Kp of 9 and minimum Dst of –422 nT. The Kp remained at severe to extreme levels (6 to 9) for 27 hours. The main phase of the storm began at 3UT on November 20 and ended at 3UT on November 22. It should be noted that the pre-storm period of the November 2003 event was not totally quiet. The Kp was ≥ 3 and ≤ 5 during November 16–19.

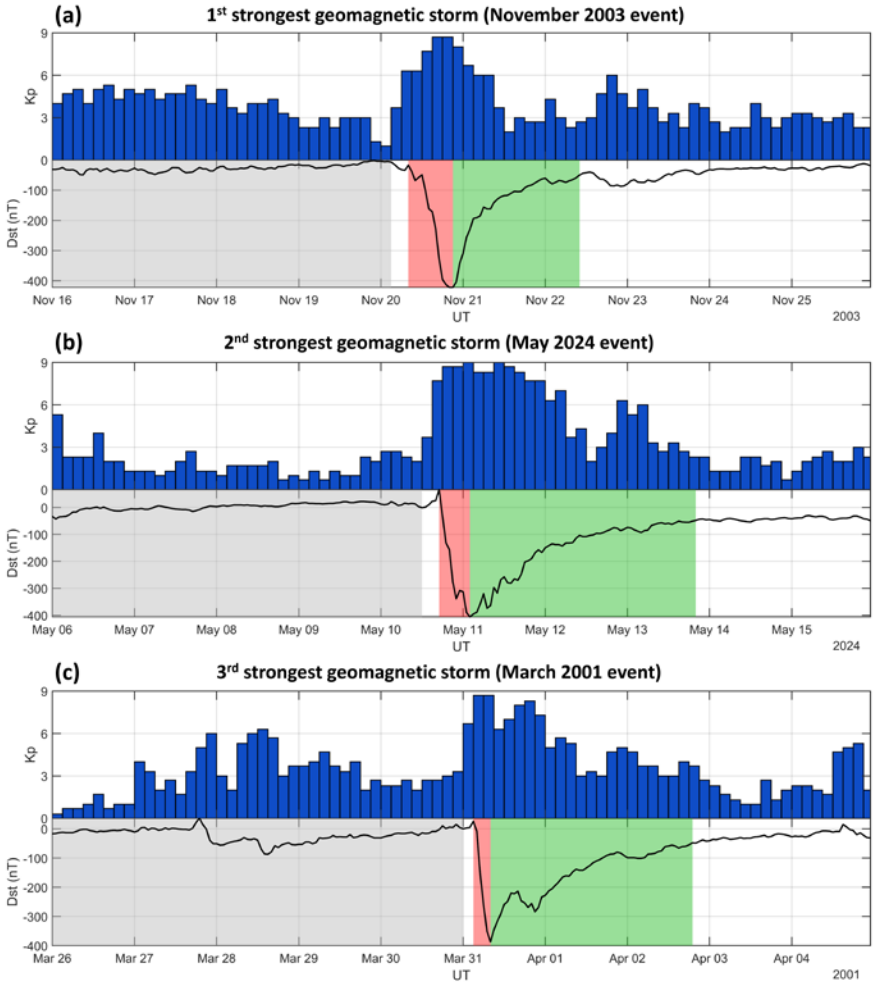

Figure 2. Kp and Dst indices during the three geomagnetic storms (the November 2003, May 2024, and March 2001 geomagnetic storms). The grey, red, and green shaded regions denote the pre-storm period, storm main phase, and storm recovery phase, respectively.

The May 2024 storm, the most recent extreme event in the Solar Cycle 25, provided a unique opportunity to assess modern GNSS infrastructure under severe space weather. The storm evolution was complex, driven by successive CMEs (Romano et al., 2024). The Dst index exhibited a two-step intensification during the main phase, eventually reaching a minimum of –412 nT at 15UT on May 11. While the magnitude of the 2024 event is slightly smaller than that of the 2003 event, however the Dst decreased more rapidly and the duration of Kp at severe to extreme levels lasted longer in the 2024 event than both 2021 and 2003 events. In addition, the pre-storm period of the 2024 event was generally quiet, with Kp values below 3 most of the time.

The March 2001 event occurred near the peak of Solar Cycle 23 and represented a classic solar maximum superstorm. The storm showed a classic profile with a clear initial phase, a deep main phase, and a gradual recovery. The Kp remained at severe to extreme levels for 24 hours. The Dst index reached a minimum of –387 nT at 8UT on March 31. The Dst of this event had the sharpest decrease among the three events. It should be noted that the pre-storm period of the March 2001 event was not completely quiet. There was a small geomagnetic storm with minimum Dst of -87 on March 27–28, 2001.

3.2 Impacts of Extreme Geomagnetic Storms on Kinematic PPP Errors

To quantitatively assess the degradation of positioning performance under extreme geomagnetic storm events, we analyzed the 3D positioning errors of kinematic PPP of all the selected IGS stations. The analysis focused on two key metrics: the Root Mean Square Errors (RMSE), which reflects the overall accuracy, and the 95th percentile (P95) error, which indicates the reliability and robustness of the solution by highlighting the large positioning errors. The RMSE of PPP positioning errors for the three storm events is shown in Figure 3, categorized by latitudes (high-latitudes, mid-latitudes, and low-latitudes) and the phase of storm (pre-storm period, storm main phase, and storm recovery phase).

The histogram reveals a similar high-latitude pattern of RMSE across all the three superstorms. During the pre-storm period of November 2003 and March 2001 events, the RMSE remained at centimeter level, typically near 7 cm. For the pre-storm period of May 2024 event, the RMSE is close to 3 cm. These centimeter level RMSE indicates that reasonably good kinematic PPP performance can be obtained under stable ionospheric conditions. During the storm main phase, a significant degradation in accuracy was observed. The RMSE raised to nearly 14 cm in November 2003 and March 2001 events. For the May 2024 event, the RMSE of main phase reached 7 cm. The positioning errors of the main phase of all the three cases increased by a factor of ~2X compared to those of the pre-storm period. During the storm recovery phase, the RMSE was slightly larger than that of pre-storm period in May 2024 and March 2001 events. For the November 2003 event, the RMSE of recovery phase was slightly smaller than that of pre-storm period. It should be noted that the RMSE of pre-storm period in November 2003 and March 2001 events were larger than that of May 2024 event for all latitudes. This maybe be related with the disturbed pre-storm period in November 2003 and March 2001 events.

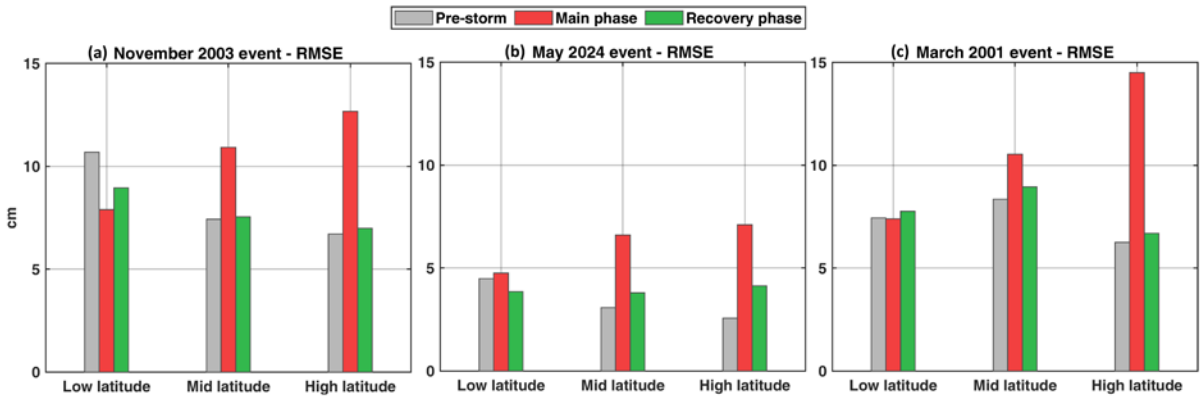

Figure 3. RMSE of GPS kinematic PPP 3D positioning errors at low-, mid-, and high-latitude GPS stations during the three geomagnetic storms (the November 2003, May 2024, and March 2001 geomagnetic storms).

Because the statistics of different latitudes showed the largest and most consistent degradation at high latitudes, the time-series analyses focus on the high-latitude station group, where storm effects were strongest. Figure 4 illustrates the time series and temporal variations of 3D RMSE positioning errors for high-latitude stations. During the quiet pre-storm period, the RMSE remained stable and low in the May 2024 event. However, during the disturbed pre-storm periods, the RMSE showed large values in the November 2003 and March 2001 events. As the main phase began, a sharp increase in RMSE was observed in all three cases, along with positioning error spike exceeding 10 cm. As the storm transitioned into recovery phase, the RMSE decreased but still exhibited some large values. These results were consistent with the statistical results seen in the histograms.

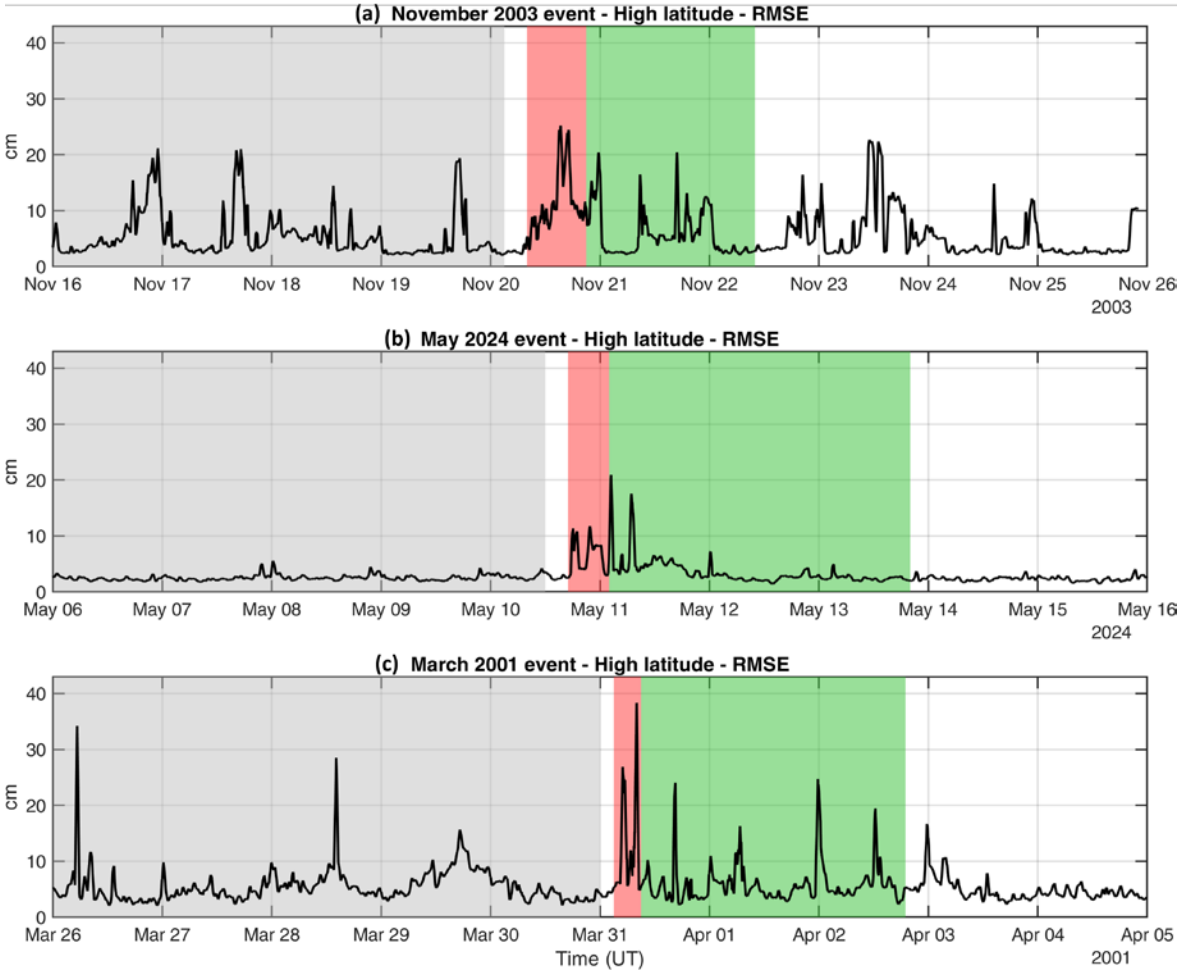

Figure 4. The high-latitude RMSE of GPS kinematic PPP 3D positioning errors during the three geomagnetic storms (the November 2003, May 2024, and March 2001 geomagnetic storms).

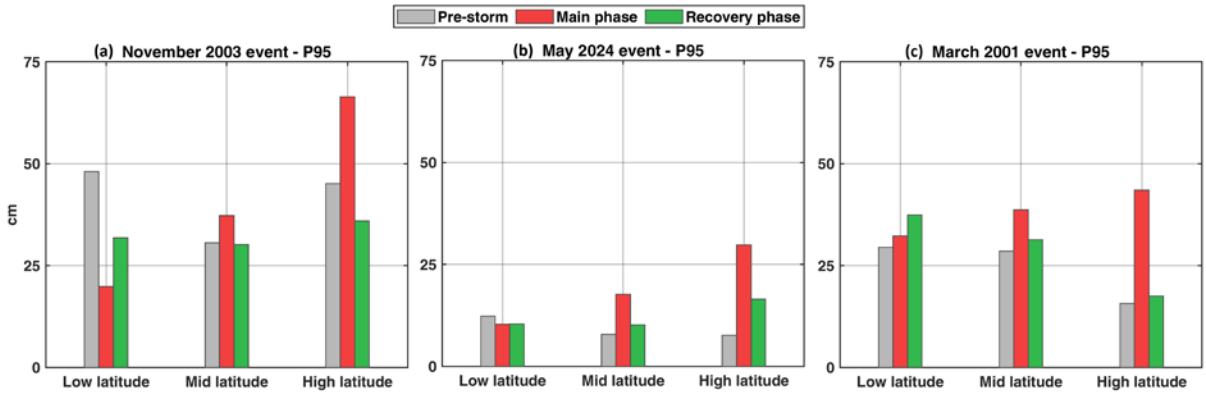

Figure 5. The P95 of GPS kinematic PPP 3D positioning errors during the three geomagnetic storms (the November 2003, May 2024, and March 2001 geomagnetic storms).

While RMSE provides a measure of average performance, the 95th percentile (P95) of positioning error gives another aspect of PPP performance. As shown in Figure 5, the P95 histogram showed an even more pronounced degradation of PPP than the RMSE at high-latitudes during main phase in March 2001 and May 2024 events. The high-latitude P95 increased by a factor of 3X, from ~15 cm during the pre-storm period to ~45 cm during the main phase in March 2001 event. For May 2024 event, the high-latitude P95 increased by a factor of 4X, from ~7 cm during the pre-storm period to ~28 cm during the main phase. It is worth noting that mid-latitude P95 increased by a factor of 2X, from ~8 cm during the pre-storm period to ~16 cm during the main phase. During the main phase of the November 2003 event, the high-latitude P95 only increased by a factor of 1.5X, from ~44 cm during the pre-storm period to ~66 cm during the main phase.

A comparative analysis of the statistical patterns provided useful insights into storm impacts. While the RMSE distribution patterns were generally similar across the three storm cases, each showing comparable overall degradation during the main phase, the P95 patterns were distinct for each event. This discrepancy showed that geomagnetic storms of similar intensity tended to produce similar average impacts on PPP positioning accuracy. However, the "worst-case scenarios" characterized by the P95 parameter revealed that each storm has its own unique characteristics. This suggests that the evolution of ionospheric irregularities and the resulting severe, localized disturbances vary considerably from event to event. These variations affect the reliability and tail risk of positioning services differently despite similar storm magnitudes.

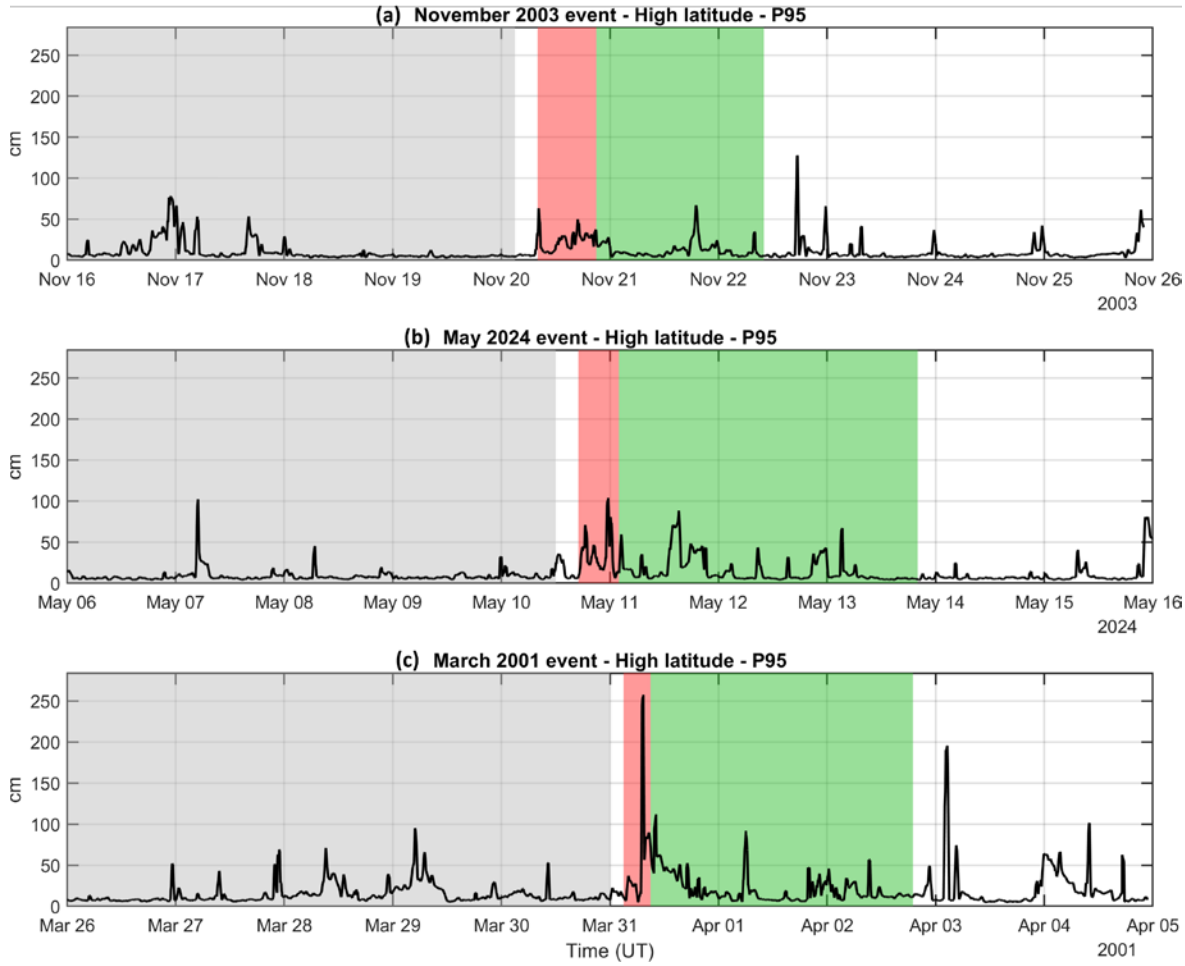

Figure 6. The time series of high-latitude P95 of GPS kinematic PPP 3D positioning errors during the three geomagnetic storms (the November 2003, May 2024, and March 2001 geomagnetic storms).

Figure 6 depicts the time series and temporal evolution of the P95 3D positioning errors for high-latitude stations. During the quiet pre-storm period, the P95 values remained relatively constrained and low in the May 2024 event. However, during the disturbed pre-storm periods in the November 2003 and March 2001 events, the P95 already exhibited elevated values. As the main phase began, a simultaneous increase in P95 was observed with error values exceeding 30 cm in November 2003 and May 2024 events. Unlike the RMSE, which reflected average degradation, the rapidly fluctuating P95 time series reveals the positioning solution was highly unreliable during main phase. As the storm transitioned into the recovery phase, the P95 showed a rapid reduction within a few hours. This indicated that although the magnetospheric or ionospheric recovery process may persist for days, the severe ionospheric irregularities responsible for extreme positioning outliers dissipated relatively quickly, allowing the reliability of the PPP service to be restored shortly after the peak of the disturbance. However, distinct spikes in P95 were still observed during the recovery phase. This phenomenon suggests that although the overall error magnitude during recovery phase is smaller than that of main phase, the occurrence of substorms can still cause sudden disturbances in the polar ionosphere, thereby threatening the reliability of PPP solutions during specific intervals.

3.3 The Impact of Extreme Geomagnetic Storms on Kinematic PPP Outage Rate

To evaluate the availability and continuity of the GPS PPP service during extreme space weather events, the PPP outage rate was calculated. In this study, an “outage” is defined as an epoch where the PPP algorithm fails to provide a coordinate solution due to an insufficient number of available satellites or a failure to estimate positioning solution. A valid epoch requires at least four healthy satellites and a position dilution of precision (PDOP) no greater than 6, the conventional threshold for adequate GPS geometry

(U.S. Department of Defense, 2020). Severe ionospheric scintillation can cause signal blockage, loss of lock, or frequent cycle slips, causing either of these requirements not to be met. The outage rate is defined as the percentage of outage epochs relative to the total observed epochs during a specific period of time.

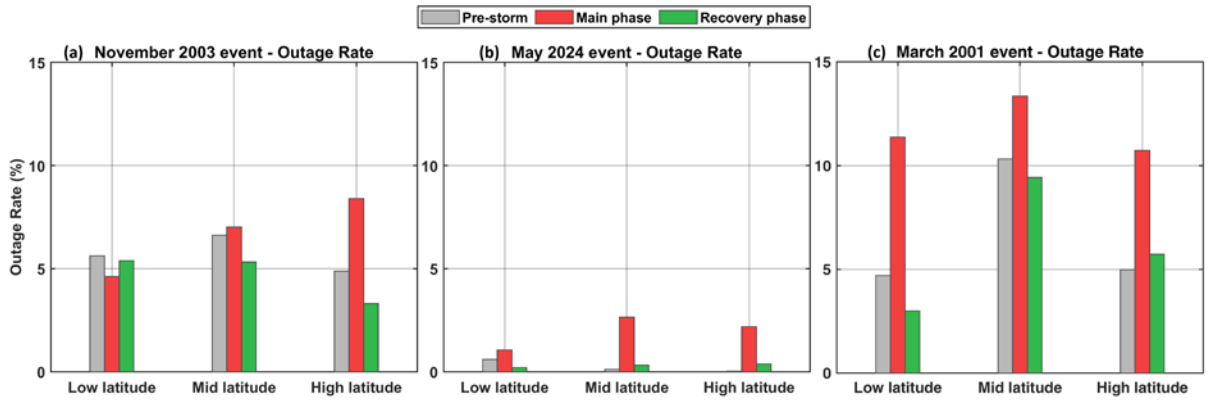

Figure 7. The outage rate of GPS kinematic PPP 3D positioning errors during the three geomagnetic storms (the November 2003, May 2024, and March 2001 geomagnetic storms).

Figure 7 illustrates the PPP outage rate at different latitudes and storm phases for the three events. For November 2003 event, the outage rate at high latitudes during the main phase was significantly larger than that during pre-storm period. In contrast to the significant degradation observed at high latitudes, the outage rates in the middle and low-latitude regions showed little difference between the pre-storm, main phase, and recovery phases. This suggests that the effects of geomagnetic storms in mid and low latitudes were not sufficiently intense to cause complete losses of positioning solution, even though they might have induced moderate ionospheric disturbances that affected positioning accuracy (as evidenced by the increased RMSE and P95 in Section 3.2). An interesting observation from the comparative analysis was that the outage rate during the May 2024 event was notably lower than that observed in the 2003 and 2001 cases, despite the 2024 event being an extreme superstorm of comparable magnitude. This improvement in service availability was likely attributable to the significant advancements in GPS satellite technology and ground receiver hardware/software over the past two decades. Modern receivers in 2024 are equipped with more sophisticated signal tracking loops and higher sensitivity, which enhance their resilience against signal fading. Furthermore, the modernized GPS constellation provides superior signal power and geometry compared to the early 2000s, effectively mitigating the risk of complete positioning outages. However, despite these improvements in receiver robustness, a significant discrepancy between the pre-storm and main phase outage rates persisted in the high-latitude region for the 2024 case. The statistics showed an increase from ~0.2% during the pre-storm phase to ~2.2% during the main phase. This increase demonstrated that even with advanced receiver technology, the extreme ionospheric irregularities resulting from the main phase of an extreme geomagnetic storm remained capable of severely compromising the continuity of PPP services in high latitude regions.

Furthermore, Figure 8 shows three co-located high-latitude stations, highlighting that the type of receiver hardware plays a pivotal role in maintaining the continuity of GPS positioning capability during geomagnetic storms. The distance between these three collocated stations (YELL, YEL2, and YEL3) is ~50 m. YELL station was equipped with a JAVAD TRE_3N DELTA receiver. YEL2 and YEL3 stations were equipped with SEPT POLARX5TR receivers. To quantify their differences over time, the time-varying outage rate was calculated using a 30-minute sliding window. At the 30-s sampling interval, each complete window contained 60 epochs, and the outage rate was computed as $N_{outage}/N_{total} \times 100\%$, where N_{outage} is the number of epochs without a valid PPP coordinate solution and N_{total} is the number of expected epochs in the window. The window was advanced by one epoch (30 s) to generate the time series. Despite experiencing almost the identical ionospheric disturbance conditions, the stations equipped with different receivers exhibited significantly different PPP outage rates. YEL2 and YEL3 stations both demonstrated a distinct performance profile compared to YELL station. The discrepancy in their outage rates underscored that resilience to ionospheric scintillation heavily depends on receiver technologies. Differences in tracking loop algorithms, signal processing strategies, and dynamic range capabilities between receiver models determine their ability to maintain signal lock and provide valid

solutions when faced with rapid phase and amplitude fluctuations.

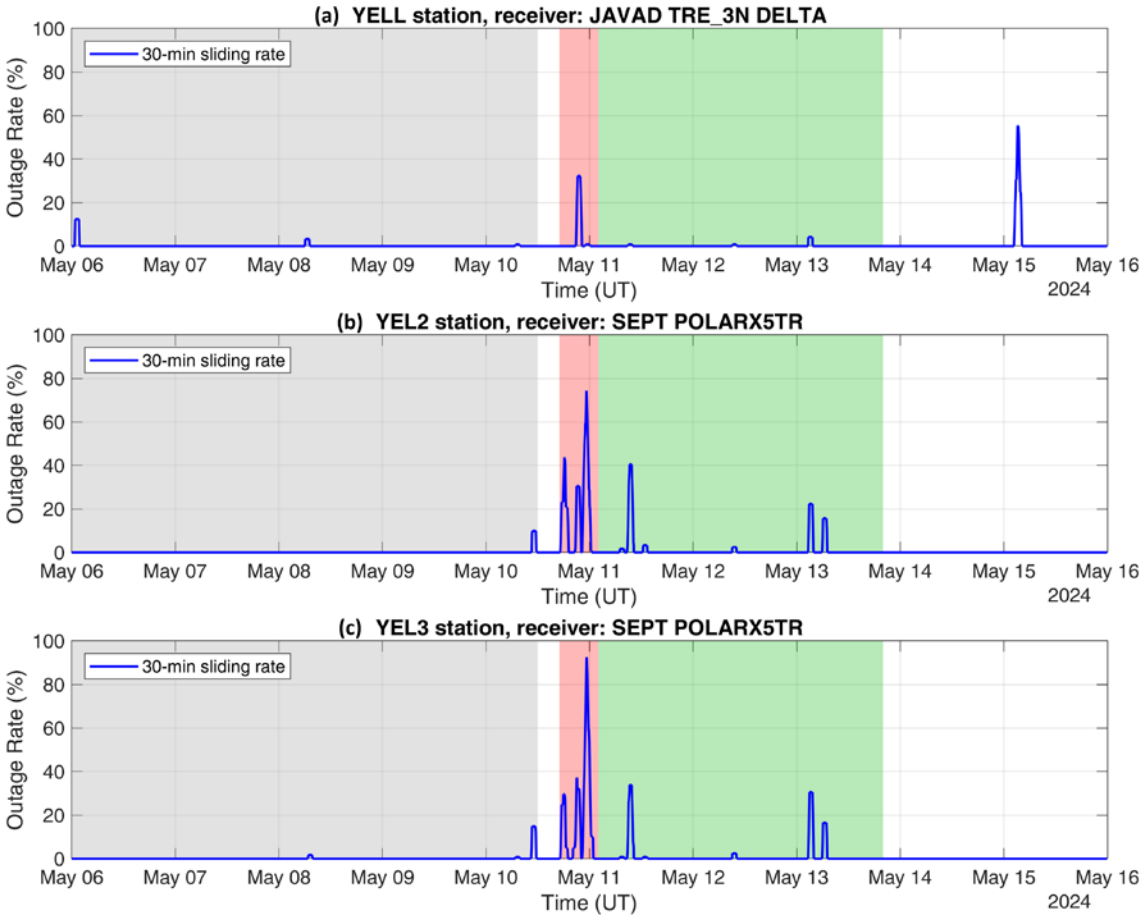

Figure 8. The outage rate of GPS kinematic PPP within a 30-minute sliding window at (a) YELL station, (b) YEL2 station, and (c) YEL3 station.

4 Discussion

The impacts of extreme geomagnetic storms on GPS positioning performance are complex and multifaceted. While this study focuses on the degradation caused by storm-induced ionospheric disturbances, it is important to acknowledge that positioning errors during these events stem from a confluence of factors, not solely the magnetic storm itself. These factors include ionospheric scintillation induced by non-storm plasma irregularities (such as equatorial plasma bubbles, EPBs), multipath effects from the local observation environment, tropospheric delay modeling errors, satellite orbit and clock inaccuracies, and inherent receiver noise. For instance, at low latitudes, the performance of PPP is frequently influenced by EPBs, a phenomenon that frequently occurs even during periods of geomagnetically quiet time. EPBs can generate intense small-scale irregularities and scintillation, leading to signal degradation similar to that observed in the auroral regions. Therefore, the specific error characteristics at low latitudes during the selected geomagnetic storm events may reflect a superposition of both storm-induced effects and other factors, complicating the direct attribution of errors to the geomagnetic storm alone.

The storm time RMSE of GPS kinematic PPP positioning errors reported here (on the order of tens of centimeters) is generally smaller than the values reported in previous storms studies of similar intensities, which often exceeded one meter (e.g., Jacobsen & Andalsvik, 2016; Yang et al., 2020). This discrepancy is likely attributed to the advancements in the processing software. In this study, we utilized the PRIDE PPP-AR, recognized as one of the best open-source software for high-precision GNSS analysis. Its superior performance in processing algorithm contributes to enhanced kinematic solutions even under disturbed conditions. This result is consistent with recent study conducted by Yang & Morton (2025), who also employed the PRIDE software to study the May

2024 event and reported error magnitudes consistent with our results. This suggests that modern GPS or GNSS processing algorithms can significantly mitigate positioning degradation, thereby improving the resilience of PPP services.

Furthermore, the comparative analysis of the three largest geomagnetic storms provides insights that single-case studies cannot offer. First, a discrepancy was observed between the patterns of RMSE and P95. While the RMSE patterns were generally similar across the three events, showing consistent degradation during the main phase, the P95 patterns were distinctly different for each storm. This indicates that while geomagnetic storms of similar intensity tend to produce comparable average impacts on positioning accuracy, the "worst-case" scenarios are highly variable. This variability suggests that the evolution of small-scale and localized ionospheric irregularities, which drive extreme outliers, is unique to each event's specific solar wind drivers and magnetosphere-ionosphere coupling dynamics. Consequently, relying solely on average accuracy metrics may underestimate the risks to safety-critical GPS applications. Second, the comparison highlights a clear evolution over time in hardware resilience. The outage rate during the May 2024 event was notably lower than those during the 2003 and 2001 events. This improvement is likely attributable to the significant technological advancements in GNSS instruments over the last two decades. Modern receivers in 2024 were equipped with advanced tracking loops and higher sensitivity, and the modernized GPS constellation provides superior signal functioning performance. These advancements enhance the system's ability to maintain signal lock and solution continuity under stress. Nevertheless, the persistence of significant degradation in high-latitude regions during the 2024 event underscores that modern GNSS infrastructure is not immune to the extreme forces of superstorms, highlighting the continued need for space weather mitigation strategies in critical applications.

5 Summary

This study presented a comparative analysis of GPS kinematic PPP performance during three largest geomagnetic storms in the last three decades: the March 2001, November 2003, and May 2024 events. By employing a consistent processing strategy with the PRIDE PPP-AR software on a global IGS station network, we evaluated degradation in terms of 3D positioning errors (RMSE and P95) and service availability (outage rate) across different latitudes and storm phases. The key findings are summarized as follows:

1. All three superstorms caused significant positioning accuracy degradation, primarily in high-latitude regions. The RMSE of GPS kinematic PPP during the main phase increased by a factor of approximately ~2X compared to the pre-storm period.

2. While RMSE distributions were similar across different events, P95 patterns were distinct. This indicates that although storms of similar intensity produce comparable average accuracy impacts, the localized extreme disturbances responsible for the "worst-case" errors are highly variable and event-specific.

3. The May 2024 event provided a unique opportunity to assess the resilience of modern GPS infrastructure to extreme geomagnetic storms. Despite having a comparable intensity to the 2001 and 2003 events, the 2024 storm exhibited a notably lower outage rate. This improvement is attributed to advancements in GPS satellite signal and modernized receiver hardware and software technologies. However, even with these technological gains, high-latitude regions still experienced a non-negligible increase in outage rates during the main phase (rising from ~0.2% to ~2.2%), underscoring that extreme space weather remains a threat to GPS service continuity.

4. The comparison among three co-located stations (YELL, YEL2 and YEL3) highlighted the critical role of receiver hardware in storm resilience. During the storm main phase, the peak 30-minute outage rates were approximately 32% at YELL, 74% at YEL2, and 92% at YEL3, demonstrating marked receiver-dependent differences under nearly identical ionospheric conditions.

In conclusion, while modern GNSS infrastructure, hardware and software have significantly enhanced the robustness of satellite positioning services against geomagnetic disturbances, vulnerabilities remain, particularly at high latitudes where ionospheric irregularities are the most intense. These results emphasize the necessity for continued development of mitigation strategies, including the selection of robust receiver hardware and the implementation of advanced monitoring algorithms, to ensure the accuracy and continuity of GPS positioning services in future solar cycles.

Acknowledgments

This work is supported by the Research Grants Council of the Hong Kong Special Administrative Region, China under projects PolyU/RGC

15221620/B-Q80Q, 15205821/B-Q84W, 15212622/B Q94L, and the Hong Kong Polytechnic University (under Projects ZH8Y and 4-ZZVL). National Natural Science Foundation of China 42530201, and National Key R&D Program of China 2025YFF0512302.

Data Availability Statement

GNSS rinex data were sourced from the International GNSS Service (IGS) at http://www.igs.org. The precise satellite ephemeris and clock products are provided by IGS Data Center of WHU (http://www.igs.gnsswhu.cn/index.php).

References

[1] Abdu, M. A. (2012). Equatorial spread F/plasma bubble irregularities under storm time disturbance electric fields. Journal of Atmospheric and Solar-Terrestrial Physics, 75–76, 44–56. https://doi.org/10.1016/j.jastp.2011.04.024

[2] Alex, S., Mukherjee, S., & Lakhina, G. S. (2006). Geomagnetic signatures during the intense geomagnetic storms of 29 October and 20 November 2003. Journal of Atmospheric and Solar-Terrestrial Physics, 68(7), 769–780. https://doi.org/10.1016/j.jastp.2006.01.003

[3] Balan, N., Li, Q., Liu, L., & Le, H. (2018). An introduction to equatorial electrodynamics and a review of an additional layer at low latitudes. Journal of Atmospheric and Solar-Terrestrial Physics, 181, 94–109. https://doi.org/10.1016/j.jastp.2018.10.011

[4] Bartels, J., Heck, N. H., & Johnston, H. F. (1939). The three-hour-range index measuring geomagnetic activity. Terrestrial Magnetism and Atmospheric Electricity, 44(4), 411–454. https://doi.org/10.1029/TE044i004p00411

[5] Danilchuk, E., Yasyukevich, Y., Vesnin, A., Klyusilov, A., & Zhang, B. (2025). Impact of the May 2024 extreme geomagnetic storm on the ionosphere and GNSS positioning. Remote Sensing, 17(9), 1492. https://doi.org/10.3390/rs17091492

[6] Elvidge, S., & Themens, D. (2024). The probability of the May 2024 solar superstorm. In Review. https://doi.org/10.21203/rs.3.rs-4780404/v1

[7] Fejer, B. G. (1997). The electrodynamics of the low-latitude ionosphere: Recent results and future challenges. Journal of Atmospheric and Solar-Terrestrial Physics, 59(13), 1465–1482. https://doi.org/10.1016/S1364-6826(96)00149-6

[8] Geng, J., Chen, X., Pan, Y., Mao, S., Li, C., Zhou, J., & Zhang, K. (2019). PRIDE PPP-AR: An open-source software for GPS PPP ambiguity resolution. GPS Solutions, 23(4), 91. https://doi.org/10.1007/s10291-019-0888-1

[9] Gonzalez, W. D., Joselyn, J. A., Kamide, Y., Kroehl, H. W., Rostoker, G., Tsurutani, B. T., & Vasyliunas, V. M. (1994). What is a geomagnetic storm? Journal of Geophysical Research: Space Physics, 99(A4), 5771–5792. https://doi.org/10.1029/93JA02867

[11] Hernandez-Pajares, M., Zornoza, J. M. J., Subirana, J. S., Farnworth, R., & Soley, S. (2005). EGNOS test bed ionospheric corrections under the October and November 2003 storms. IEEE Transactions on Geoscience and Remote Sensing, 43(10), 2283–2293. https://doi.org/10.1109/TGRS.2005.855625

[12] Jacobsen, K. S., & Andalsvik, Y. L. (2016). Overview of the 2015 St. Patrick's Day storm and its consequences for RTK and PPP positioning in Norway. Journal of Space Weather and Space Climate, 6, A9. https://doi.org/10.1051/swsc/2016004

[13] Kamide, Y., Baumjohann, W., Daglis, I. A., Gonzalez, W. D., Grande, M., Joselyn, J. A., McPherron, R. L., Phillips, J. L., Reeves, E. G. D., Rostoker, G., Sharma, A. S., Singer, H. J., Tsurutani, B. T., & Vasyliunas, V. M. (1998). Current understanding of magnetic storms: Storm-substorm relationships. Journal of Geophysical Research: Space Physics, 103(A8), 17705–17728. https://doi.org/10.1029/98JA01426

[14] Kelley, M. C. (1989). High-latitude electrodynamics. In The Earth's ionosphere (pp. 261–310). Elsevier. https://doi.org/10.1016/B978-0-12-404013-7.50011-3

[15] Li, Z., Wang, N., Liu, A., Yuan, Y., Wang, L., Hernández-Pajares, M., Krankowski, A., & Yuan, H. (2021). Status of CAS global ionospheric maps after the maximum of solar cycle 24. Satellite Navigation, 2(1), 19. https://doi.org/10.1186/s43020-021-00050-2

[16] Liu, B., Liu, J., Liu, X., Zhong, J., Li, S., & Li, Q. (2023). Dynamics of thermospheric traveling atmospheric disturbance during a geomagnetic storm. Journal of Geophysical Research: Space Physics, 128(8), e2023JA031448. https://doi.org/10.1029/2023JA031448

[17] Liu, B., Liu, L., Liu, A., Yang, Y., Zhao, X., Li, Z., Yue, X., Liu, J., Le, H., Chen, Y., Zhang, R., & Li, W. (2026). Study of regional ionospheric structures and their impacts on SPP and PPP with multi-instrument observations in the Asian sector. Satellite Navigation, 7(1), 5. https://doi.org/10.1186/s43020-026-00191-2

[18] Lu, Y., Wang, Z., Ji, S., & Chen, W. (2020). Assessing the positioning performance under the effects of strong ionospheric anomalies with multi-GNSS in Hong Kong. Radio Science, 55(8), e2019RS007004. https://doi.org/10.1029/2019RS007004

[19] Park, J., Spogli, L., Azeez, A., Alfonsi, L., Cesaroni, C., Romano, V., & Akande, A. (2025). The impact of Mother's Day storms in May 2024 on precise point positioning at mid-latitudes. Annals of Geophysics, 68(2), A214. https://doi.org/10.4401/ag-9161

[20] Romano, P., Elmhamdi, A., Marassi, A., & Contarino, A. L. (2024). Analyzing the sequence of phases leading to the formation of the active region 13664, with potential carrington-like characteristics. The Astrophysical Journal Letters, 973(1), L31. https://doi.org/10.3847/2041-8213/ad77cb

[21] Sojka, J. J., Rice, D., Eccles, J. V., Berkey, F. T., Kintner, P., & Denig, W. (2004). Understanding midlatitude space weather: Storm impacts observed at bear lake observatory on 31 march 2001. Space Weather, 2(10), 2004SW000086. https://doi.org/10.1029/2004SW000086

[22] Stankov, S. M., Warnant, R., & Stegen, K. (2009). Trans-ionospheric GPS signal delay gradients observed over mid-latitude Europe during the geomagnetic storms of October–November 2003. Advances in Space Research, 43(9), 1314–1324. https://doi.org/10.1016/j.asr.2008.12.012

[23] Tanskanen, E. I., Slavin, J. A., Tanskanen, A. J., Viljanen, A., Pulkkinen, T. I., Koskinen, H. E. J., Pulkkinen, A., & Eastwood, J. (2005). Magnetospheric substorms are strongly modulated by interplanetary high-speed streams. Geophysical Research Letters, 32(16), 2005GL023318. https://doi.org/10.1029/2005GL023318

[24] Tsurutani, B. T., & Gonzalez, W. D. (1997). The interplanetary causes of magnetic storms: A review. In B. T. Tsurutani, W. D. Gonzalez, Y. Kamide, & J. K. Arballo (Eds.), Geophysical monograph series (Vol. 98, pp. 77–89). American Geophysical Union. https://doi.org/10.1029/GM098p0077

[25] Tsurutani, B. T., Gonzalez, W. D., Gonzalez, A. L. C., Guarnieri, F. L., Gopalswamy, N., Grande, M., Kamide, Y., Kasahara, Y., Lu, G., Mann, I., McPherron, R., Soraas, F., & Vasyliunas, V. (2006). Corotating solar wind streams and recurrent geomagnetic activity: A review. Journal of Geophysical Research: Space Physics, 111(A7), 2005JA011273. https://doi.org/10.1029/2005JA011273

[26] U.S. Department of Defense. (2020). Global Positioning System Standard Positioning Service Performance Standard (5th ed.). https://www.gps.gov/sites/default/files/2025-07/2020-SPS-performance-standard.pdf

[27] Wang, N., Li, Z., Yuan, Y., & Huo, X. (2021). BeiDou global ionospheric delay correction model (BDGIM): Performance analysis during different levels of solar conditions. GPS Solutions, 25(3), 97. https://doi.org/10.1007/s10291-021-01125-y

[28] Wang, R., Gao, J., Yao, Y., Sun, P., & Wan, M. (2020). Assessment of the algorithm for single frequency precise point positioning at different latitudes and with distinct magnetic storm conditions. Applied Sciences, 10(7), 2268. https://doi.org/10.3390/app10072268

[29] Wernik, A. W., Secan, J. A., & Fremouw, E. J. (2003). Ionospheric irregularities and scintillation. Advances in Space Research, 31(4), 971–981. https://doi.org/10.1016/S0273-1177(02)00795-0

[30] Warnant, R., Kutiev, I., Marinov, P., Bavier, M., & Lejeune, S. (2007). Ionospheric and geomagnetic conditions during periods of degraded GPS position accuracy: 2. RTK events during disturbed and quiet geomagnetic conditions. Advances in Space Research, 39(5), 881–888. https://doi.org/10.1016/j.asr.2006.06.018

[31] Yang, Z., & Morton, Y. T. J. (2025). Impacts of the May 2024 extreme geomagnetic storm on global high-accuracy GPS positioning solutions. Space Weather, 23(10), e2025SW004547. https://doi.org/10.1029/2025SW004547

[32] Yang, Z., Morton, Y. T. J., Zakharenkova, I., Cherniak, I., Song, S., & Li, W. (2020). Global view of ionospheric disturbance impacts on kinematic GPS positioning solutions during the 2015 St. Patrick's Day storm. Journal of Geophysical Research: Space Physics, 125(7), e2019JA027681. https://doi.org/10.1029/2019JA027681

[33] Zakharenkova, I., & Cherniak, I. (2021). Effects of storm-induced equatorial plasma bubbles on GPS-based kinematic positioning at equatorial and middle latitudes during the September 7–8, 2017, geomagnetic storm. GPS Solutions, 25(4), 132. https://doi.org/10.1007/s10291-021-01166-3

[34] Zhang, J., Richardson, I. G., Webb, D. F., Gopalswamy, N., Huttunen, E., Kasper, J. C., Nitta, N. V., Poomvises, W., Thompson, B. J., Wu, C.-C., Yashiro, S., & Zhukov, A. N. (2007). Solar and interplanetary sources of major geomagnetic storms (Dst $\leqslant$ -100 nT) during 1996–2005. Journal of Geophysical Research:

Space Physics, 112(A10), 2007JA012321. https://doi.org/10.1029/2007JA012321
[35] Zhang, S., He, L., & Wu, L. (2020). Statistical study of loss of GPS signals caused by severe and great geomagnetic storms. Journal of Geophysical Research: Space Physics, 125(9), e2019JA027749. https://doi.org/10.1029/2019JA027749
[36] Zhang, Z., Wang, N., Liu, A., Li, Z., Li, A., Wang, L., & Zhang, Y. (2025). Assessing 1-second ROTI for ionospheric perturbation monitoring using real-time multi-GNSS data in China. Space Weather, 23(2), e2024SW004187. https://doi.org/10.1029/2024SW004187
[37] Zumberge, J. F., Heflin, M. B., Jefferson, D. C., Watkins, M. M., & Webb, F. H. (1997). Precise point positioning for the efficient and robust analysis of GPS data from large networks. Journal of Geophysical Research: Solid Earth, 102(B3), 5005–5017. https://doi.org/10.1029/96JB03860

Authors



Zhizhao Liu is a Full Professor in the Department of Land Surveying and Geospatial Science (LSGS) at The Hong Kong Polytechnic University (PolyU), Hong Kong, China. He concurrently serves as Chief Scientist at the Meteorological Observation Center of the China Meteorological Administration (CMA), Scientific Advisor to the Hong Kong Observatory (HKO), and Adjunct Professor at the University of Calgary, Canada. Prof. Liu is the Founding President of the Hong Kong Chapter of the Canadian Institute of Geomatics (CIG) and served as President of the International Association of Chinese Professionals in Global Positioning Systems (CPGPS) in 2013.

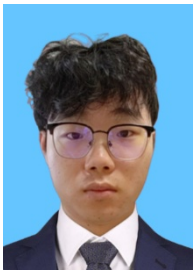

The Micro-Laboratory of Atmospheric Research and Geomatics Engineering (Micro-LARGE) Prof. Liu founded in 2009 has achieved international acclaim for pioneering innovations and developing widely adopted algorithms spanning satellite navigation, atmospheric remote sensing, and numerical weather prediction (NWP), such as multi-frequency GNSS cycle slip detection/repair, "non-physical calibration models" that improve satellite water vapor retrieval accuracy by 20% to 60%. His Lab claimed to be the second research entity globally (after the UK Met Office) to successfully assimilate near-infrared satellite water vapor into NWP models (March 2023). His Lab is also the first one to study the economic impact of space weather on civil aviation, earning recognition from NASA JPL senior researcher and a highlight in Nature Reviews Earth & Environment.

Prof. Liu has spearheaded several milestone observational systems, including China's first GPS PPP-based real-time precipitable water vapor monitoring system in the Pearl River Delta (PRD), Hong Kong's first GNSS-based ionospheric scintillation monitoring network (2012), and Hong Kong's first collocated GNSS-radiosonde water vapor sounding system in partnership with the HKO (2013). More recently, he has partnered with the Hong Kong Observatory (HKO) to deploy his Lab's Hong Kong Water Atmospheric Vapor Estimation System (HK-WAVES), enhancing HKO's operational capabilities in extreme weather forecasting.

Prof. Liu received the inaugural Early Career Award from the Hong Kong Research Grants Council (RGC, 2012), the inaugural Best Paper Award at the China Satellite Navigation Conference (CSNC, 2013), and was nominated by HKO for the WMO Norbert Gerbier-MUMM International Award (2015). He received his B.Sc. in Surveying Engineering from Jiangxi University of Science and Technology (1994), M.Sc. in Geodesy from Wuhan University (1997), and Ph.D. in Geomatics Engineering from the University of Calgary (2004).

Bowei Liu received his bachelor's degree from Shandong University. He is currently a Ph.D. candidate at the Institute of Geology and Geophysics, Chinese Academy of Sciences, and the University of Chinese Academy of Sciences. He worked as a research assistant at The Hong Kong Polytechnic University. His research focuses on ionospheric physics, GNSS-based ionospheric observations, and the impacts of space weather on satellite navigation systems.



Jing WU received the B.E. degree in Geomatics from Chang'an University, Xi'an, China, and the M.S. degree from the Chinese Academy of Sciences (CAS), She is currently pursuing the Ph.D. degree at The Hong Kong Polytechnic

University. Her current research interests in GNSS precise point positioning (PPP).



Libo Liu received his Ph.D. degree from Wuhan University. He is a professor at the Institute of Geology and Geophysics, Chinese Academy of Sciences, and the University of Chinese Academy of Sciences. He is also affiliated with the Heilongjiang Mohe National Observatory of Geophysics. His research focuses on solar-terrestrial physics, ionospheric dynamics, ionospheric modeling, and the responses of the ionosphere to solar and geomagnetic activities.



Biqiang Zhao received his Ph.D. degree from Wuhan Institute of Physics and Mathematics, Chinese Academy of Sciences. He is a professor at the Institute of Geology and Geophysics, Chinese Academy of Sciences, and the University of Chinese Academy of Sciences. His research interests include low-latitude ionospheric dynamics, ionospheric fine-scale structures, ionospheric weather and climate variability, and their impacts on space weather.